Theoretical and Computational Fluid Dynamics manuscript No.
(will be inserted by the editor)

Roel Neggers · Bjorn Stevens · J. David Neelin

A simple equilibrium model for shallow cumulus convection

In preparation: August 17, 2005

Abstract A new equilibrium model for shallow cumulus topped mixed layers is presented. A variant on the w_* closure for the shallow cumulus mass flux is applied which retains the convective area fraction in its formulation. As opposed to being constant the fraction is explicitly modeled, using a statistical closure as a function of the saturation deficit and humidity variance at cloud base. As a consequence, important new interactions are introduced between convective transport, humidity and depth of the mixed layer. This mechanism, which we call the mass flux - humidity feedback, helps determine the character of the equilibrium state such that mixed layer top is maintained close to cloud base height. Due to the strong sensitivity of the mass flux to the area fraction, the latter thus acts as a regulator or valve mechanism on moist convective transport. As a consequence, the mixed layer model is able to explain the robustness of many aspects of the shallow cumulus boundary layer that is typically found in observations and large-eddy simulations (LES).

The model is evaluated for a single LES case as well as for global climatology obtained from a 40 year reanalysis of meteorological data by the European Centre for Medium-range Weather Forecasts (ECMWF). LES characteristics of convective mass flux, cloud fraction, humidity variance, cloud base height and surface fluxes of heat and humidity are reproduced. The solution on reanalysis fields reproduces the spatial structure of mixed layer temperature and humidity and their associated surface fluxes in the subtropical Atlantic and Pacific Tradewind areas. Furthermore, the spatial structure of the convective area fraction matches that of synoptic surface observations of frequency of occurrence of shallow cumulus. Particularly striking is the smooth onset of the convective area fraction and mass flux along the Tradewind trajectory that is reproduced, from zero to typical Tradewind values. The cumulus onset represents the necessity for shallow cumulus mass flux to occur in order to close the mixed layer budgets of heat, moisture and mass, as a response to the changing magnitude of large scale subsidence and free tropospheric humidity along the trajectory. Finally, as an a posteriori test, the mass flux closure was implemented in an intermediate-complexity tropical climate model, to study it when coupled to the large scale flow. A climate run then shows that the mass flux - humidity feedback acts to keep the shallow cumulus boundary layer close to its equilibrium state for long, climatological timescales.

Keywords Atmospheric Boundary Layer · Shallow Cumulus · Mass flux · Equilibrium

R. A. J. Neggers · B. Stevens · J. D. Neelin
Department of Atmospheric and Oceanic Sciences,
University of California at Los Angeles (UCLA)

R. A. J. Neggers
Current affiliation: European Centre for Medium-range Weather Forecasts (ECMWF)
Shinfield Park, Reading, Berkshire, RG2 9AX, United Kingdom
Tel.: +44-118-9499607
Fax: +44-118-9869450
E-mail: Roel.Neggers@ecmwf.int

1 Introduction

The budgets of heat and humidity in the steady state marine shallow cumulus boundary layer result from a delicate balance among surface heat and moisture fluxes, dry and moist convective transport, radiation, and transport by the large-scale flow [30,39,27]. The exact state of the associated shallow cumulus cloud population is an expression of this balance. For example, moist convective mass flux dominates vertical transport, strongly affecting the thermodynamic state of the boundary layer. Yet cloud occurrence necessary for moist convection in turn strongly depends on humidity conditions. As a consequence, explaining cloud occurrence requires a proper understanding of the interactions and feedbacks between all processes that lead to the observed equilibrium state.

The shallow cumulus boundary layer has been the subject of many research efforts, using a variety of observations, theoretical models, and general circulation models. Several equilibrium models have been formulated for marine cloudy boundary layers, for stratocumulus [21,31] as well as for shallow cumulus [1,8,9]. The emergence of large-eddy simulation (LES) modelling has greatly contributed to shallow cumulus research, as it provides a high-resolution three-dimensional representation of the boundary layer, explicitly resolving the most energetic scales of motion. An intriguing result of LES research has been the robustness of the shallow cumulus mass flux, cloud fraction and surface fluxes to model formulation and resolution [36,11,32]. This robustness suggests that some mechanism exists that is efficient in pushing the system to a certain equilibrium state [17].

This study has the purpose of identifying and modelling the dominant feedbacks that lead to the observed equilibrium state of the shallow cumulus boundary layer. While shallow cumulus research has typically focused on processes in the cloud layer, the interaction of this type of convection with the subcloud mixed layer [8] has received less attention. Yet it can be argued that this interaction is key to establishing the equilibrium state. The balance in the mixed layer budgets of temperature and humidity is, with constant large scale forcings, mainly controlled by only two processes: the surface flux and the convective flux at cloud base. The surface flux is usually formulated in a bulk approach, which simply acts to restore the subcloud humidity and temperature to the values at the surface on a timescale set by the speed of the surface wind and the depth of the subcloud layer. This passive behaviour implies that the main process that is actively responsible for setting the final equilibrium balance has to be convection. Accordingly, this justifies focussing our attention on the cloud base convective flux in particular.

In the last decades several important findings have been made that are relevant for our purposes. The mass flux approach [29,7,39] has been shown by Siebesma and Cuijpers [34] to effectively capture the cloud base convective flux in shallow cumulus. The mass flux is by definition the product of a vertical velocity scale and a convective area fraction. Observational data [26] and numerical results [18,23] have shown that the relevant vertical velocity scale at cloud base is the convective vertical velocity scale of the subcloud layer [15]. The Gaussian statistical formulation [35] is successful in reproducing LES cloud fractions at cloud base [13]. Here knowledge is required of the local saturation deficit as well as the second statistical moment of turbulence, the variance. At mixed layer top the latter scales [24] with properties of the cloud base transition layer [5,1,40], in particular the local vertical gradients, the cloud base convective flux, and the turnover timescale of the subcloud layer.

This study presents a new equilibrium model for a marine shallow-cumulus-topped mixed layer in which some of these recent insights are combined. The system of equations is closed using a formulation for the mass flux that retains the area fraction of the active, surface driven cloudy thermals in its formulation [23]. Letting the area fraction depend on the state of the system (as opposed to a constant) introduces feedbacks that better maintain the height of the boundary layer near lifting condensation level. The area fraction is modeled using a statistical formulation, as a function of humidity and variance at cloud base. It will be shown that these feedbacks help determine the character of the equilibrium. Comparison to observations, LES and reanalysis data shows that the shallow cumulus mass flux, convective area fraction, cloud base height, mixed layer thermodynamic state and variances, and surface fluxes associated with this equilibrium are realistic. In order to optimize transparency only a simplified boundary layer scenario is studied. This is sufficient to reveal the mechanisms of interest.

In Sections 2 the model is formulated. In Section 3 the details of the large scale forcings, boundary conditions and constants are given that are used to solve the model. In Section 4 the model is solved at a single point using a shallow cumulus case designed for LES, and over a field of forcings derived from the 40 year reanalysis of meteorological data by the European Centre for Medium-range Weather

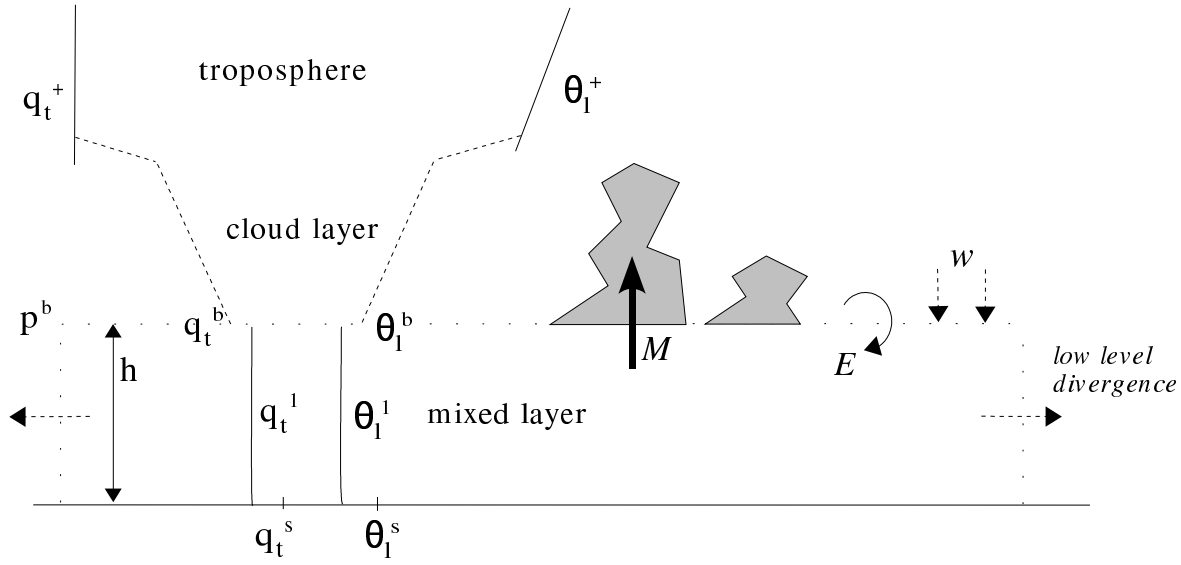

Fig. 1 An idealized view of a shallow cumulus topped boundary layer. The symbols are explained in the text.

Forecasts (ECMWF). The results are evaluated against LES results as well as observed Tradewind climatology of shallow cumulus occurrence and cloud base height. A timeseries analysis is performed to illustrate the relaxation towards equilibrium, revealing the role of the new humidity - mass flux feedback in this process. This mechanism is put in context of previous equilibrium models for shallow cumulus [1,8]. Finally, as an a posteriori test the mass flux model is implemented in an intermediate complexity climate model in which it is fully coupled to larger scale dynamics. The model used to this purpose is the Quasi-equilibrium Tropical Circulation Model (QTCM, see [22]). In Section 5 the implications of the results are further discussed, and in Section 6 the conclusions are summarized.

2 Model formulation

Figure 1 shows a schematic view of the atmospheric boundary layer, featuring a well-mixed subcloud layer topped by a conditionally unstable shallow cumulus cloud layer. These layers are defined by the vertical stucture of the mean profiles of liquid water potential temperature θ_l and total specific humidity q_t [7]. Between the two layers, $\{q_t, \theta_l\}$ exhibit a small jump associated with the transition layer, situated in between mixed layer top and cloud base height. This transition layer at cloud base is typically observed in the vertical structure of shallow cumulus topped boundary layers, especially in the humidity profile [5,1,40]. Surface values are indicated by the superscript s, mixed layer values by 1, cloud base values by b, and free tropospheric values by $+$. Various physical processes affecting the mixed layer humidity, heat and mass budgets are represented in the figure.

2.1 Subcloud mass budget

Mass conservation in the steady state mixed layer below the clouds can be expressed as

$$\frac{\partial h}{\partial t} = E + w - M = 0 \tag{1}$$

where h is the height of the mixed layer, w is the large-scale vertical velocity at h (positive upwards), E is the top entrainment velocity, and M is the shallow cumulus mass flux at cloud base. The transition layer is here considered an integral part of the bulk mixed layer, to the purpose of making M "drain" the bulk layer as a whole. Although the depth of the transition layer (i.e. the distance between mixed layer top and cloud base height) is thus not explicitly modeled here, it is still implicitly accounted for through the cloud base mass flux closure, as will be illustrated later. w represents the mass-tendency

due to lateral outflow at the column edges by low level divergence of the large scale winds, pushing down the stable transition layer at h. Integrating the divergence of the horizontal winds D over the mixed layer implies

$$w \;=\; -\,D\,h, \tag{2}$$

see [37] for a detailed derivation and approximations. The cumulus mass flux M acts as a sink term in the mixed layer mass budget. In contrast, E is a source term, representing the process of engulfment of cloud layer air into the mixed layer. Equating the buoyancy flux $\overline{w'\theta_v'}$ at h as the product of E and the vertical jump in virtual potential temperature $\theta_v = \theta(1 + 0.61q_t - 1.61q_l)$ gives

$$E \;=\; -\,\frac{\overline{w'\theta_v'}\big|_h}{\Delta\theta_v} \;=\; \frac{0.2\,\overline{w'\theta_v'}\big|_s}{\Delta\theta_v}, \tag{3}$$

The script h refers to mixed layer top, while $\Delta(..) = (..)^b - (..)^1$ stands for the jump over the transition layer. Here the buoyancy flux at h is equated as a fixed negative factor of the surface buoyancy flux. Equation (3) is the standard definition of top entrainment for dry convective boundary layers, and is shown by [32,36] to be similar in the presence of shallow cumulus clouds. Finally, $\Delta\theta_v$ can be expressed in terms of $\{\Delta q_t, \Delta\theta_l\}$,

$$\Delta\theta_v \;=\; \Delta\theta_l \;+\; 0.61\left(\; q_t^1\Delta\theta_l \;+\; \theta_l^1\Delta q_t \;+\; \Delta q_t\Delta\theta_l \;\right), \tag{4}$$

where is assumed that no liquid water exists in the (cloud free) areas where top entrainment occurs. This relation illustrates that typically both jumps contribute oppositely to stability.

In steady state situations, mixed layer height h is such that top entrainment exactly balances the loss of mass by cumulus mass flux and large scale divergence. Shallow cumulus cloud base height in the Trades is observed to be typically robust and rather constant at about 500-700m, but to gradually increase along the Tradewind trajectory towards the tropics [30].

2.2 Simplified budget equations

The subcloud layer is assumed to be well-mixed for temperature and humidity. The most important sources and sinks in their budgets in the mixed layer are the surface flux, the flux at mixed layer top, the large scale forcings, and in case of temperature the radiation [37]. Accordingly, the simplified vertically integrated prognostic budget equations can be written as

$$h\,\frac{\partial q_t^1}{\partial t} \;=\; V\,C_q^s\,\left(q_t^s \;-\; q_t^1\right) \;+\; E\,\Delta q_t \;+\; h\,F_{\mathrm{adv}_{q_t}}, \tag{5}$$

$$h\,\frac{\partial \theta_l^1}{\partial t} \;=\; V\,C_\theta^s\,\left(\theta_l^s \;-\; \theta_l^1\right) \;+\; E\,\Delta\theta_l \;+\; h\,F_{\mathrm{adv}_{\theta_l}} \;+\; h\,F_{\mathrm{rad}}. \tag{6}$$

Here V is the horizontal wind speed close to the surface, and C_q^s and C_θ^s are the bulk transfer coefficients at the surface. The F terms stand for large-scale forcings, where *adv* indicates horizontal advection and *rad* radiative processes.

The downward flux at mixed layer top in (5)-(6) is formulated as the product of the entrainment velocity scale E times the jump in humidity and temperature between mixed layer and cloud layer. This jump is assumed here to be a function of the total difference between mixed layer and free troposphere,

$$\Delta q_t \;\approx\; C_q^c\,\left(q_t^+ \;-\; q_t^1\right), \tag{7}$$

$$\Delta\theta_l \;\approx\; C_\theta^c\,\left(\theta_l^+ \;-\; \theta_l^1\right), \tag{8}$$

where the superscript + indicates the free tropospheric value overlying the boundary layer. The coefficients C_q^c and C_θ^c are transfer coefficients characteristic for the downward transport of free tropospheric air through the cloud layer. Equations (7)-(8) represent a simple linear model for this process. This ensures that the air entrained into the mixed layer is still affected by the properties of its mixing source. For the moment, the cloud layer transfer coefficients C_q^c and C_θ^c are set constant, and are tuned to give reasonable solutions. Our main purpose with this model is to explore to what degree subcloud mixed layer budgets alone can explain the boundary layer equilibrium state, so inclusion of a more complex cloud layer transport model is considered future work for the moment.

	V [m s^{-1}]	SST [K]	D [10^{-6} s^{-1}]	q_t^+ [g kg^{-1}]	θ_l^+ [K]	F_{rad} [K day^{-1}]	$F_{\text{adv}\theta_l}$ [K day^{-1}]	$F_{\text{adv}q_t}$ [g kg^{-1} day^{-1}]
BOMEX	8.75	300.4	4.3	4.0	308	-2.0	0.0	-1.2

Table 1 Characteristics of the BOMEX marine shallow cumulus case input parameters used to solve the equilibrium model. The LES case description is given by [32].

The appearance of E in the budget equations (5)-(6) reflects the fact that mass transport by M and w conceptually does not change mixed layer humidity and potential temperature. Extraction of air out of the well-mixed bulk layer does not affect the average over the remaining air. Accordingly, only top-entrainment of air out of the overlying cloud layer into the mixed layer and the subsequent mixing process can change q_t^1 and θ_l^1. However, note that the mass flux and large scale subsidence still appear in the model in the mass budget (1).

2.3 Mass flux closure

In order to complete the system of prognostic equations (1), (5) and (6) the cloud base mass flux M must be parameterized. The commonly used mass flux approach [7] states that the turbulent flux by cumulus can be well approximated by

$$\overline{w'\phi'} \;=\; M\;\left(\phi^{up} \;-\; \overline{\phi}\right). \tag{9}$$

Here ϕ stands for $\{q_t, \theta_l\}$, the superscript up indicates the air of the rising moist updrafts, and the vertical bar stands for a horizontal average. The mass flux M is the product of an area fraction and a velocity scale,

$$M \;\equiv\; a^c w^c, \tag{10}$$

where a_c is the area fraction of the transporting cloudy thermals and w_c is their vertical velocity scale. For simplicity the air density ρ is assumed to be constant, $\rho = 1$ kg m^{-3}.

The average vertical velocity over all buoyant, cloudy thermals (named the "cloud core") was shown by [23] to scale well with the Deardorff convective velocity scale w^*, defined as

$$w^c \;\approx w^* \;\equiv\; \left(\frac{g\;h}{\Theta_v^0}\,\overline{w'\theta_v'}\Big|_s\right)^{\frac{1}{3}}. \tag{11}$$

The surface buoyancy flux $\overline{w'\theta_v'}\big|_s$ can be expressed in terms of the surface heat and moisture fluxes [14], which in the bulk aerodynamic formulation are a function of q_t^1 and θ_l^1.

Based on GATE observations [26] suggests that M is proportional w^*. The same conclusions are drawn in [18] from a TKE budget analysis, introducing a constant of proportionality 0.03 obtained from LES simulations. However, retaining the area fraction a^c in the mass flux closure instead of a constant permits one to distinguish between conditions where a larger or smaller fraction of the active mixed-layer thermals associated with w_* actually condensate, and thus contribute to M [23]. This connection with mixed layer humidity could be essential in enabling a realistic equilibrium solution for this system of equations. As a first-order guess for the convective area fraction at the top of the mixed layer, a simplified version of the statistical cloud fraction parameterization of [13] is used that only acts on moisture,

$$a^c \;=\; 0.5 \;+\; \beta\;\text{Atan}\left(\gamma\frac{q_t^1 - q_{sat}(T,p^b)}{\sigma_q}\right). \tag{12}$$

where q_{sat} is the saturation specific humidity and p^b is the pressure at cloud base. The ratio between the brackets is the normalized saturation deficit, or the distance from saturation normalized by the turbulent variance. Since this cloud fraction is used in the mass flux, it includes only cloudy points that contribute to vertical transport. Any passive cloudiness would have to be treated separately.

	h [m]	M [m s^{-1}]	a^c [%]	w^* [m s^{-1}]	σ_q^b [g kg^{-1}]	$(q_t - q_{sat})^b$ [g kg^{-1}]	L [W m^{-2}]	H [W m^{-2}]
Model	614.6	0.038	5.89	0.65	0.65	-1.16	137	3.1
LES	620	0.022	3.5	0.51	0.64	-1.51	150	10

Table 2 Results on the BOMEX marine shallow cumulus case, comparing the simple model to LES. The LES results are averages over a range of different codes as reported by [32], except for the cloud base saturation deficit and the humidity variance which were obtained using only the KNMI LES model [14]. The cloud fraction in LES is defined as the ratio of the cloudy area to the total area at cloud base height.

For shallow cumulus convection, the humidity variance σ_q at mixed layer top has been shown by [24] to scale as

$$\sigma_q^2 = \frac{\overline{w'q'}\big|_s}{w^*} \left| q_t^1 - q_{sat} \right| \frac{h}{\Delta z} \tag{13}$$

This relation applies for situations with small convective cloud fraction, typical for shallow cumulus. Transition layer depth Δz is assumed to be constant for simplicity. Next to the convective vertical velocity scale w_*, the humidity variance is the second important parameter that couples the shallow cumulus mass flux to the subcloud layer turbulence intensity. Equally important is that the cloud base variance carries transition layer properties [24].

3 Forcings and boundary conditions

The model consists of three prognostic equations (1),(5) and (6) for $\{h, q_t^1, \theta_l^1\}$. The diagnostic variables in the model are $\{E, M, a^c, w_*, q_{sat}, \sigma_q, \Delta\theta_v, \overline{w'\theta_v'}\big|_s, \overline{w'q'}\big|_s\}$. What remains are either constants or can be considered to be large scale forcings or boundary conditions.

Firstly, the model is solved for an approximately steady state marine shallow cumulus case that has been designed for LES. This enables evaluation of the equilibrium model solution for parameters such as the cloud base mass flux and convective cloud fraction, which can only be provided by LES. The case used here is based on the Barbados Oceanic and Meteorological Experiment (BOMEX), as described by [19] and [27]. The cumulus clouds were observed to be shallow, and the boundary layer was in steady state. The BOMEX LES intercomparison case is described by [32], and an overview of the input values used here is given in Table 1.

Next the model will be solved on global climatological fields of the forcings and boundary conditions. The global input fields used here are obtained from the ECMWF Re-Analysis project (ERA40) archive. The required forcings and boundary conditions are $\{q_t^s, \theta_l^s, q_t^+, \theta_l^+, V, D, F_{\text{adv}q_t}, F_{\text{adv}\theta_l}, F_{\text{rad}}\}$. The fields q_t^s and θ_l^s can be determined given the sea surface temperature (SST) and the surface pressure (p_s). q_t^+, θ_l^+ are diagnosed at a level which is always just above the Tradewind inversion (level 47, at $\approx$ 2km), in order to avoid the presence of boundary layer properties in the climatological average. V is the 10m wind speed, and the large scale divergence D at level 51 ($\approx$ 0.75km) is used, which is assumed to be close to mixed layer top. Finally, the forcing tendencies $F_{\text{adv}q_t}$, $F_{\text{adv}\theta_l}$ and F_{rad} are obtained at level 55 ($\approx$ 0.3km). These forcings are especially important for a realistic heat budget, as they represent the only cooling term in the subcloud mixed layer (as opposed to the surface heat flux and the convective flux).

What remains is the choice of the constants $\{\Delta z, C_q^s, C_\theta^s, C_q^c, C_\theta^c\}$. These constants are set to typical values obtained from LES or observations. Δz is set to 150m [8,24]. The surface bulk transfer coefficients C_q^s and C_θ^s have the typical oceanic value of 0.0012, based on observational data [16] and often used for numerical modelling [3,38]. The constants C_q^c and C_θ^c are set to be 0.1 and 0.03 respectively, chosen after a sensitivity test for these parameters. These particular values give the best overall solution.

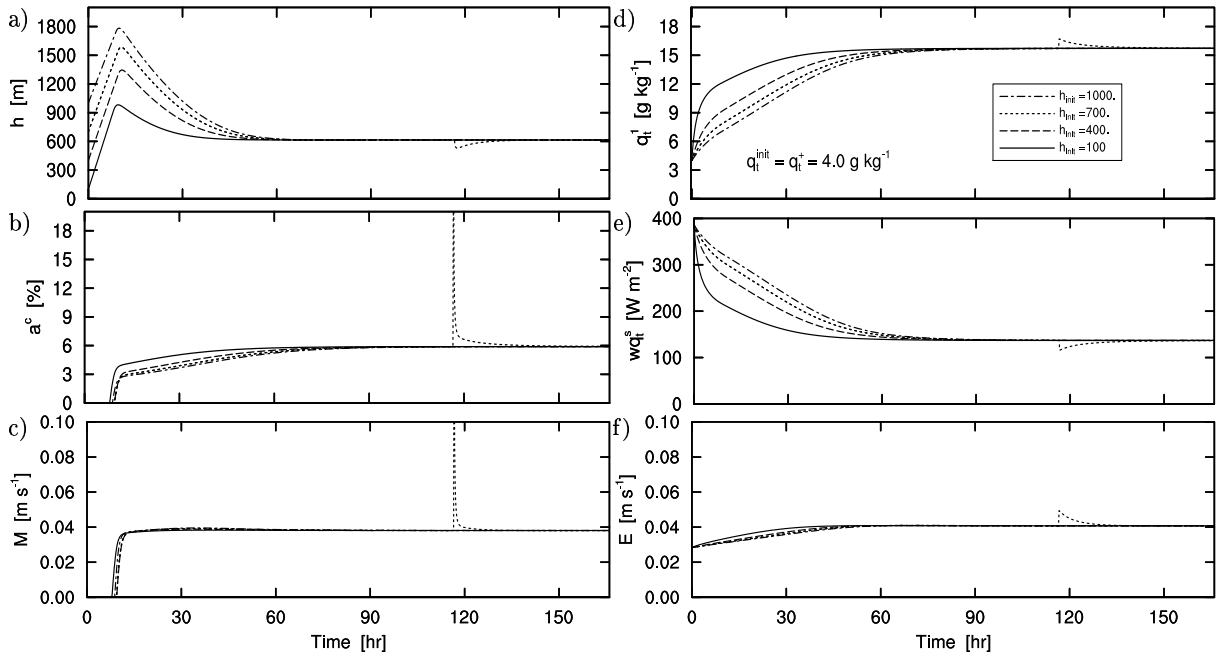

Fig. 2 Timeseries of some model variables during the solution process for the BOMEX case. a) Mixed layer depth, b) area fraction, c) mass flux, d) mixed layer humidity, e) surface evaporation, and f) entrainment rate.

4 Equilibrium solutions

The main novelty of this model is that the convective area fraction in the mass flux formulation is retained, which introduces an extra degree of freedom in the mass flux, representing new interactions between mixed layer humidity and the convective transport. Through the mass budget these might help maintain boundary layer height. As will be illustrated in this Section this humidity dependence of the convective mass flux is essential for a realistic equilibrium state of the shallow cumulus topped boundary layer, including temperature and humidity, their surface fluxes, the convective area fraction and mass flux, and the turbulent variances. The existence of such a solution has been shown by [8,1,9], and has long been suspected based on i) the observed persistence of shallow cumulus cloud occurrence in the subtropical Trades [28] and ii) the robustness of the shallow cumulus mass flux under changes in resolution and subgrid scale models in numerical large eddy simulations [17]. By putting the model in context of previous shallow cumulus equilibrium models [8,1] it will be shown that retaining a flexible convective area fraction in the mass flux as a function of humidity in fact is an alternative representation of some essential aspects of these models.

4.1 The BOMEX case

First the model is solved for the BOMEX case, using an integration timestep of 60s. Table 2 shows the model state after 167 hrs when it has equilibrated. Included are the cloud base mass flux and cloud fraction, cloud base height, convective vertical velocity scale, cloud base humidity variance and saturation deficit, and the surface fluxes of heat and moisture. LES results on the same parameters are also given.

The equilibrium state of all free model variables is of at least the right order of magnitude. The surface latent heat flux and boundary layer height have realistic values. The small convective area fraction typical for shallow convection is reproduced, as well as the mass flux and variance. The typical scatter in these variables over all LES models in the BOMEX intercomparison case [32] was about 1% in the cloud base core fraction, and 0.0075ms^{-1} in the cloud base mass flux. Judged along those criteria the equilibrium model is doing reasonably well, given that the model only represents an idealized

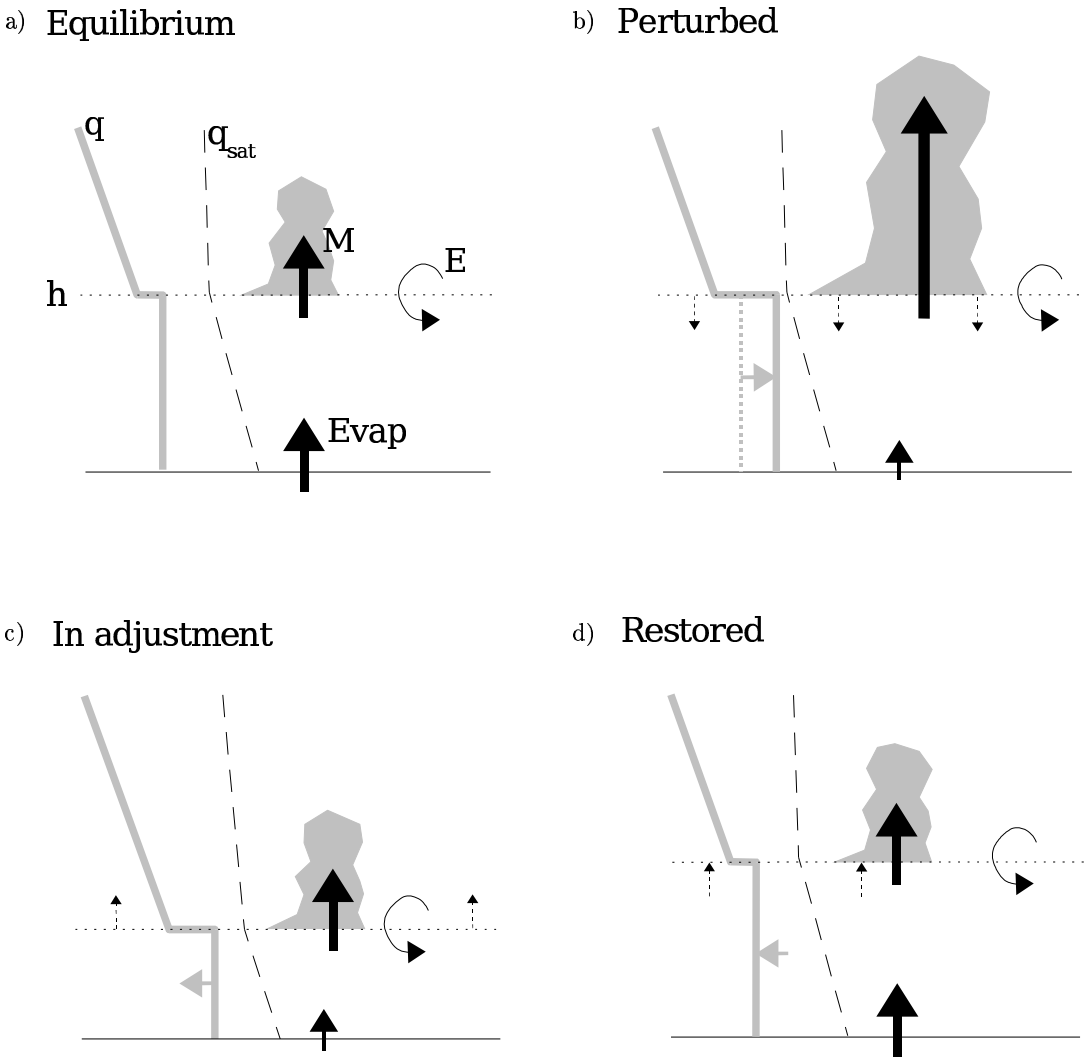

Fig. 3 Schematic illustration of the feedback mechanisms between mixed layer humidity, convective mass flux, and mixed layer height. a) The system in equilibrium; b) the state immediately after a positive humidity perturbation which yields a large M and a fast decrease in h; c) the adjustment stage in which M is restored but the mixed layer slowly gains mass by entrainment; and d) the fully restored equilibrium state. The symbols are explained in the text.

bulk mixed layer. But perhaps it is most relevant to view these results in the context of the typical unsatisfactory performance of many single column models for these parameters, as documented by several intercomparison studies on such cumulus cases [20].

Apparently the mixed layer budgets of mass, heat and humidity can explain the equilibrium state in LES of the structure of the Tradewind boundary layer, in particular the convective mass flux and cloudy area fraction. An important observation is that the equilibrium state is always close to saturation, with a typical convective area fraction at cloud base of only a few percent. This reflects that the existence of a non-zero mass flux requires the condensation of *at least some* rising thermals, due to its dependence on the area fraction.

To further explore the role of this humidity sensitivity of the mass flux, the process of adjustment to equilibrium is now studied for the BOMEX case, see Fig. 2. A sensitivity test is done on the initial boundary layer height to assess stability. Initial mixed layer humidity is always equal to q_t^+. In addition, to further assess stability a humidity perturbation of $+1$g kg^{-1} is applied at $t = 117$ hr. The results indicate that the model always reaches a stable state. First the mixed layer deepens by top entrainment, as there is no mass flux to compensate it because q_t^1 is still too small. When

finally humidity has increased such that saturation is reached at h, the mass flux quickly gets large and overcomes top entrainment to reduce h towards its equilibrium value. Full equilibrium is reached after about 100 hours, which is comparable to the model of [1].

In contrast to mixed layer depth and humidity, the area fraction a^c and mass flux M restore very quickly after the mixed layer humidity perturbation at $t = 117$ hr. Cloud base height plays an important role in this process, as illustrated schematically in Fig. 3. The reduction of h by the M perturbation affects q_{sat} at h through the associated increased temperature. This quickly increases the saturation deficit again, which restores a^c and with it M. After that, h is slowly restored by top entrainment, and humidity is slowly restored by i) the reduced surface evaporation and ii) the increased top entrainment. The only modest reduction in h expresses the robustness of the system for perturbations in humidity.

The importance of this interaction between mass flux, mixed layer humidity and cloud base height for the boundary layer equilibrium was already realized by [8] and [1]. In both models cloud base height is assumed to be close to or at the top of the well mixed layer, a constraint then used for closure of the cloud base mass flux. The analogy with this model is that here, through the area fraction, the mass flux automatically adjusts to bring h to a height where a certain fraction of rising thermals condensate such that M exactly balances E and w in the mass budget (1). This means that in equilibrium the mixed layer top will always be close to lifting condensation level, or in other words, the system automatically seeks the proximity of saturation at the top of the mixed layer. Accordingly, the non-constancy of the convective area fraction in the mass flux is an alternative expression of the constraint used by [8,1] for mass flux closure. The extra degree of freedom in the mass flux represented by the area fraction thus acts as a regulator or "valve" on convective transport, dependent on bulk mixed layer humidity conditions.

It is possible to estimate the associated adjustment timescales. In absence of cloudy mass flux the relevant timescale of the mass budget is

$$\tau_E \;=\; \frac{h}{E} \;=\; \frac{h}{w} \;=\; \frac{1}{D}, \tag{14}$$

e.g. [37]. Using BOMEX values gives $\tau_h \;=\; 2.5 \cdot 10^5$ s, about 70 hours. This is the time associated with the creation of a mixed layer by top entrainment, and can be identified in Fig. 2 as the typical timescale of adjustment of h to equilibrium after initialization, and of its restoration by entrainment after perturbation. The timescale of the sudden drop in cloud base height h' by M during the humidity perturbation is

$$\tau_M \;=\; \frac{h'}{M} \tag{15}$$

Estimating $h' \;\approx\; 100$ m and $M \approx 0.1$ m s^{-1} from Fig. 2 gives $\tau_M \;=\; 1000$ s. This is on the order of a single eddy turnover timescale, defined as

$$\tau_{eddy} \;=\; \frac{h}{w_*}. \tag{16}$$

Comparing τ_M and τ_{eddy} to τ_E shows that the mass flux acts much faster on h than the slow adjustment by top entrainment. This reflects the strong sensitivity of the mass flux to humidity through the area fraction, and the associated strong impact on the mixed layer mass budget. In Fig. 2 this is evident in the fast growth in M after cloud onset at $t = 10$ hr and its relatively strong perturbation at $t = 117$ hr. Assuming that (15) and (16) represent the same process, this gives

$$a^c \;\sim\; \frac{h'}{h} \tag{17}$$

where we substituted the definition of mass flux (10). This relation shows that retaining the area fraction in M and keeping mixed layer height close to cloud base represent the same process, as explained in words in the paragraph above. The derivation of relation (17) from first principles is given by [24].

4.2 ERA40 global fields

Next the model is solved over ocean points given the global ERA40 climatology of the boundary conditions and forcings, for the month of July. This should reproduce the characteristic spatial structure

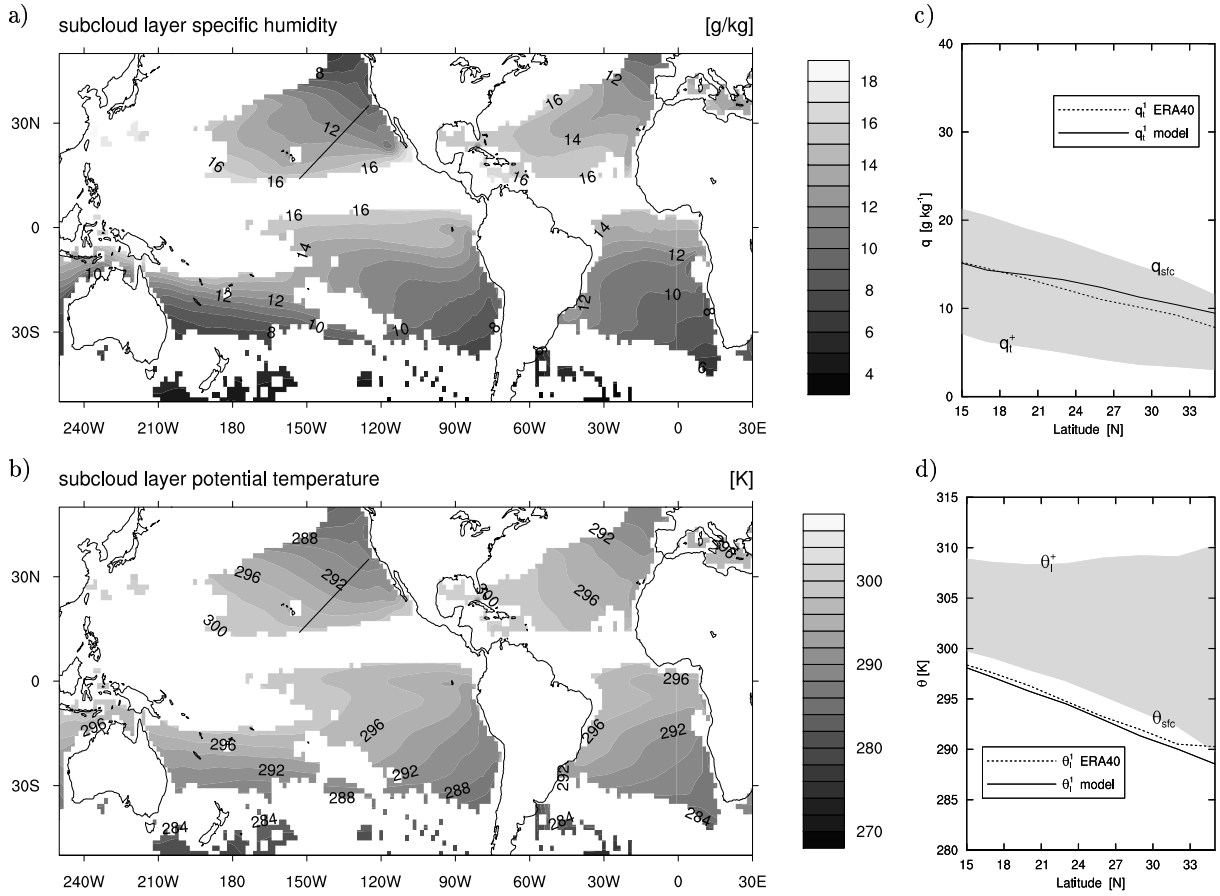

Fig. 4 The equilibrium solution with ERA40 July forcings and boundary conditions of the subcloud layer thermodynamic state, with a) total specific humidity q_t^1 and b) liquid water potential temperature θ_l^1. Panels c) and d) show a cross-section through panels a) and b) along the North-Eastern Pacific Tradewind trajectory (dark line). The boundary conditions at the surface and free troposphere are also shown (the range between these values is shaded gray), as well as ERA40 climatology of the solution variables.

and distribution of the shallow cumulus mass flux and cloud fraction. Note that the solution of the equilibrium model will only make sense in the regions in which climatology is typically dominated by shallow cumulus convection. Naturally, the subtropical oceanic Tradewind regions are the prime example, and accordingly the evaluation of the model solution will be focused on these areas. In areas where precipitation or radiative cloud top cooling play an important role the model does not capture all necessary physics, such as the intertropical convergence zone or the stratocumulus regions, respectively. Furthermore, the model will only be solved on gridpoints that have large scale subsidence, as the small jump at h has to be maintained. Finally, the model solution will only be calculated over the oceans, as over the continents the shallow cumulus boundary layer is typically not in steady state but experiences a strong diurnal cycle.

Figure 4 shows the equilibrium solution of the thermodynamic state variables q_t^1 and θ_l^1. Mixed layer temperature and humidity in the subtropics increase towards the equator, due to the increasing SST and tropospheric humidity. The solution is also plotted on a cross-section approximately aligned to the low-level Tradewinds in these areas, see Fig. 4c) and d). This cross-section is the same as used in the European Cloud-system Studies (EUROCS) intercomparison project for general circulation models on clouds in this area, as described by [33]. In general, the subcloud mixed layer temperature and humidity closely follow the ERA40 climatology. While q_t^1 is always enveloped between q_t^s and q_t^+, θ_l^1 is always lower than the surface value. This reflects that while for humidity the surface and top flux act as a source and sink respectively, they are both a source term for temperature. This is characteristic

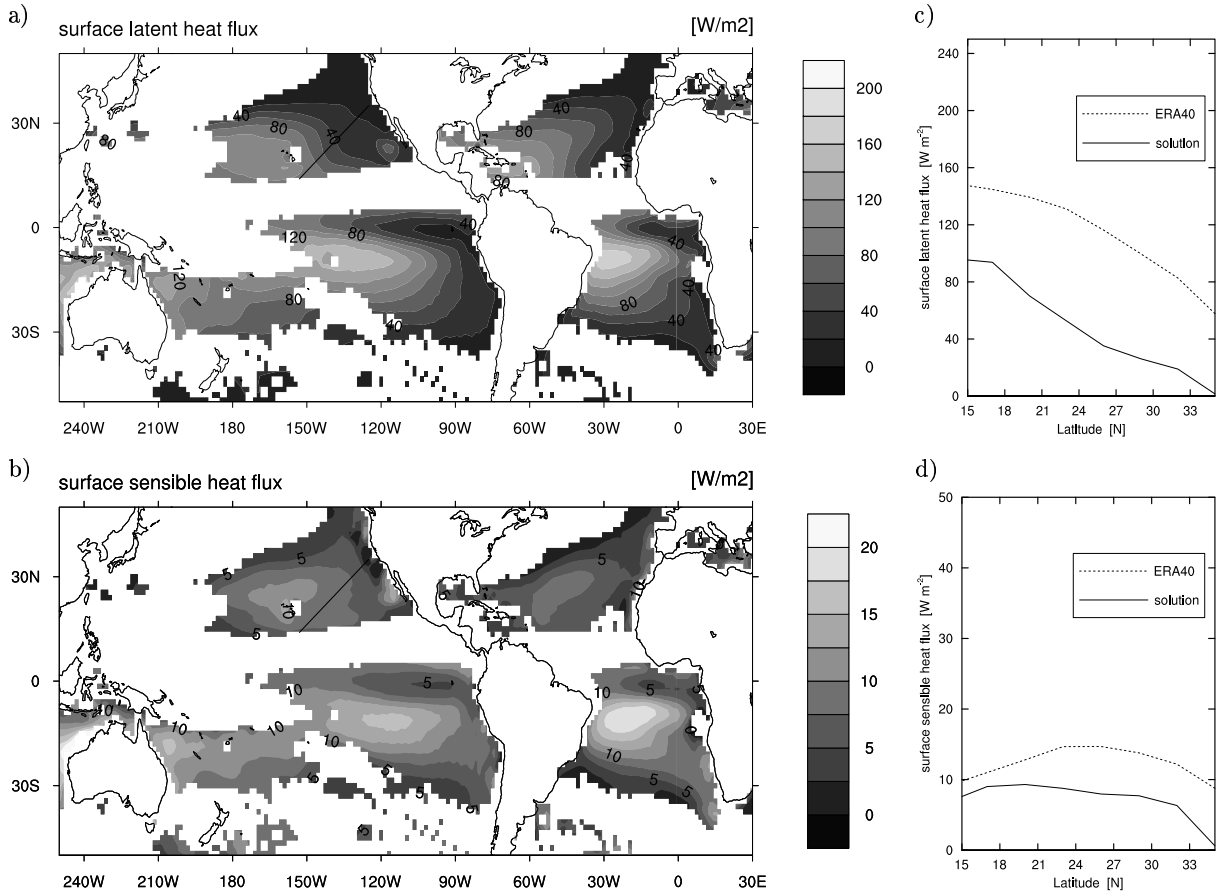

Fig. 5 The equilibrium solution with ERA40 July forcings and boundary conditions, for a) surface latent heat flux and b) surface sensible heat flux. Panels c) and d) show the cross-section through panels a) and b) along the North-Eastern Pacific Tradewind trajectory.

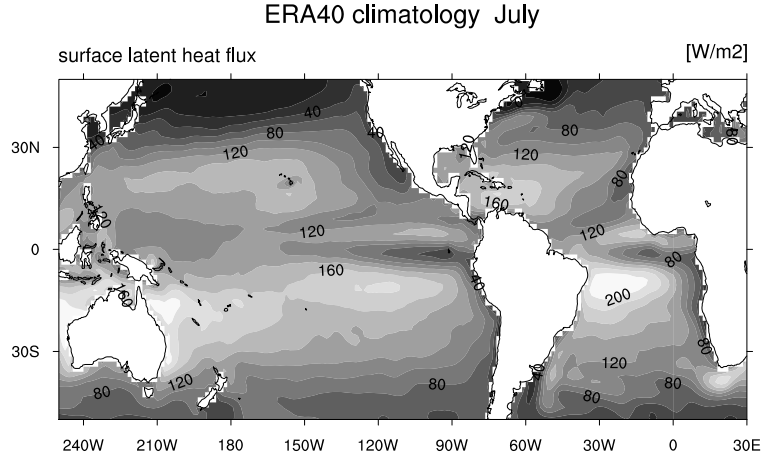

Fig. 6 ERA40 July climatology of the surface latent heat flux. Land area has been masked for convenience.

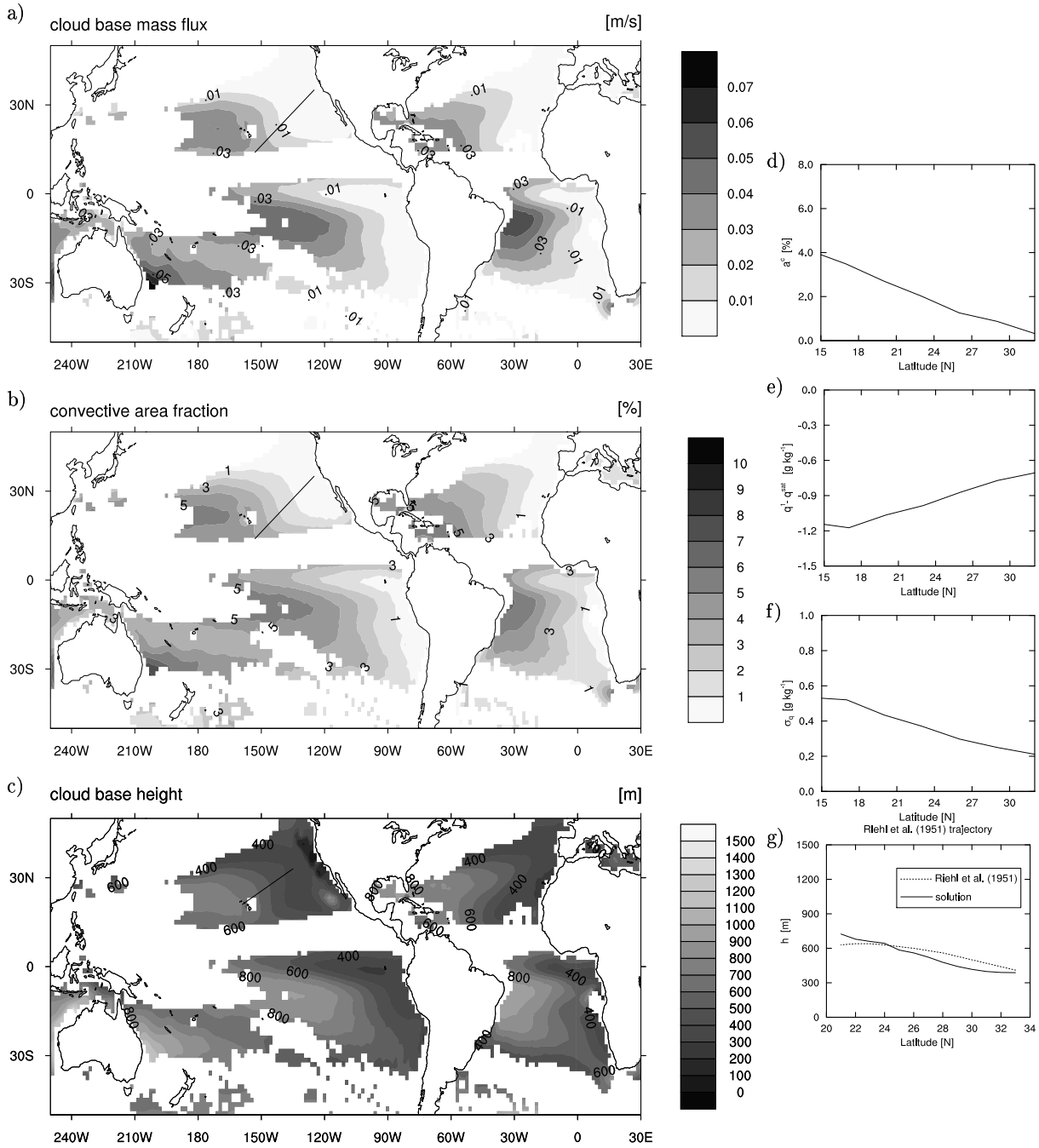

Fig. 7 The equilibrium solution with ERA40 July forcings and boundary conditions of the cloud state at cloud base, for a) mass flux, b) convective area fraction and c) cloud base height. Panels d) to g) show the cross-section along the North-Eastern Pacific Tradewind trajectory of d) convective area fraction a^c, e) saturation deficit, f) square-root of the humidity variance σ_q, and g) cloud base height. The latter is shown on a slightly differently oriented cross-section in order to compare to the cloud base height observations of [30] (dotted line).

for convective mixed layers that are only cooled by radiation and large scale advection, an aspect reproduced by the model everywhere.

The surface fluxes of sensible and latent heat are a critical indicator of model performance, as they act on small differences of temperature and humidity respectively. Figures 5a) and b) show the solution fields of the surface latent and sensible heat flux. The surface evaporation increases along the Tradewind trajectory while the sensible heat flux field is much flatter, with a maximum near Hawaii. Figures 5c) and d) show that notwithstanding a mean bias the spatial structure of the reanalysis surface latent and sensible heat fluxes is reproduced satisfactorily. The underestimation could be due to i) simplifications in the model or ii) transients in the reanalysis fields (e.g. deep convective events or surface wind bursts), not captured by the shallow cumulus model but possibly responsible for increasing the time-average surface fluxes in the reanalysis. Nevertheless, most important is that the agreement on the general spatial structure is significant, see also Figure 6.

The equilibrium solution of the cloudy state is shown in Fig. 7 a) to c). The solution fields are relatively smooth. Cloud base height is robust, always at about $400 - 800$ m but slowly increasing along the Tradewind trajectory. This is in agreement with the radiosonde observations as presented by [30], see Fig. 7g). Along the Tradewind trajectory the convective area fraction and mass flux fields feature a smooth onset, after which they slowly increase to typical Tradewind values.

Observations of cloud climatology in the Trades are typically only available in the form of frequency of occurrence, for example as obtained from in situ surface observations [28]. There is no simple relation between ship observed frequency of occurrence and area fraction. Qualitatively, however, regions of higher or lower frequency of occurrence should correspond to larger or smaller area fraction. At this qualitative level, the spatial structure of the two time-averaged signals can still be compared. Comparing Fig. 7b to the observed climatology of shallow cumulus cloud occurrence of [28] as plotted in Fig. 8 we see that there is good agreement on the basic features of the field, such as the slowly increasing shallow cumulus activity along the Tradewind flow. Considering the areas where a solution is calculated, the location of the maxima in the four Tradewind regions of the northern and southern Atlantic and Pacific oceans correspond well.

The nature of the increasing cloud fraction (and mass flux) along the Tradewind trajectory can be explored more thoroughly. Figure 7g) and h) show the two variables that determine the area fraction. Along the trajectory the humidity variance σ_q^2 increases while the saturation deficit increases too. This corresponds to a drier but more vigorously turbulent subcloud layer. Apparently stronger variance overcomes the effect of the lower relative humidity, which leads to the increasing area fraction. This turbulent structure is needed for the equilibrium between boundary layer convection and the large scale forcings and boundary conditions to be established. This is an important new aspect of the model, which results directly from the use of a statistical closure for the convective area fraction.

4.3 An interactive climate experiment

The results so far have shown that the formulation of the mass flux closure yields a realistic equilibrium. This feature makes the closure attractive for application in convection schemes for general circulation models. As an a posteriori test, the shallow cumulus mass flux scheme (9)-(13) is implemented in a larger scale tropical model. This allows the convection model to fully interact with the large-scale dynamics. A climate run is performed, and the results are compared to the model equilibrium solution and observations.

For these purposes we use the Quasi-equilibrium Tropical Circulation Model (QTCM), as formulated by [22]. This is an intermediate complexity model, featuring some key assumptions on the vertical structure of the tropical atmosphere. The resulting reduced number of degrees of freedom in the governing equations makes time integration fast, and physical processes more transparent. This is convenient for studying the interaction of experimental boundary layer convection schemes with the large scale circulation.

Compared to the standard model as described by [22] the model has been equipped with an extra degree of freedom for humidity, representing an atmospheric boundary layer of constant depth. The associated decoupling of boundary layer and free tropospheric humidity is controlled by the local intensity of atmospheric convection. The Betts-Miller scheme for deep convection as used in the standard model is expanded to cover for shallow convection as well, using a flexible shallow adjustment timescale

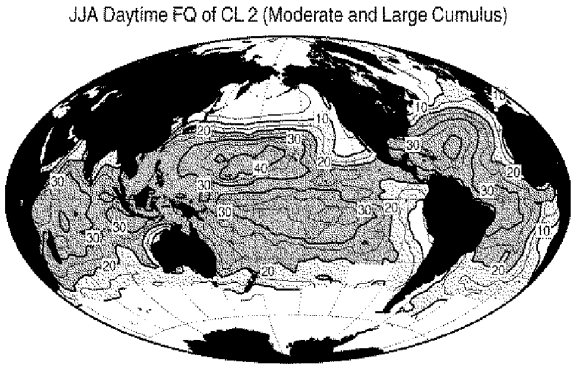

Fig. 8 Low cumulus cloud occurrence (percent) for June-August, obtained from surface synops observations. Figure reproduced from [28]. The figure represents over 60 million observations over the global oceans made between 1954-1992.

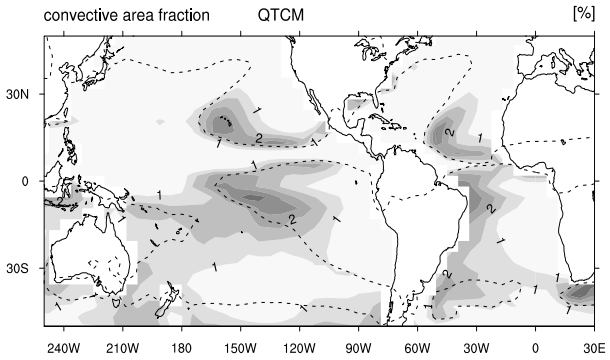

Fig. 9 July shallow cumulus convective area fraction [%] of the QTCM climate run featuring the shallow convective mass flux scheme (9)-(13). The climatological monthly mean for July is shown. The dotted line is the 70W m^{-2} precipitation rate isoline, enclosing the area where precipitating deep convection dominates in the QTCM.

dependent on the local mass flux intensity. The latter is parameterized using (9)-(13). Details of the modified QTCM and its shallow convection scheme are described by [25].

A climate run of 17 years is performed, using observed SSTs from 1981 to 1998. Figure 9 shows the resulting monthly mean July climatology of the QTCM shallow convective area fraction. The structure of the field is similar to the observed frequency of occurrence (Fig. 8) and the equilibrium model solution (Fig. 7 b). As for the equilibrium model, the QTCM implementation does not apply the shallow cumulus scheme in convective precipitative conditions, in which the standard Betts-Miller scheme is used. The mean 70 W m^{-2} contour, marked in the figure, encloses the area where the equilibrium solution is often not relevant. Note that this area is oriented somewhat differently compared to Figs 4, 5 and 7 due to the presence of transients on weather system timescales, yielding alterations between precipitation and shallow convection. There are also slight differences in climatology of convergence in the QTCM compared to ERA40. The agreement between the QTCM and the equilibrium model in the solution areas shows that in this a-posteriori test the mass flux model retains its favorable behaviour. It does not cause instability in the larger scale model, but rather keeps the boundary layer state close to the observed equilibrium state, for long climatological timescales. In addition, the representation of the surface fluxes is greatly improved. For a detailed QTCM study of the impact of shallow cumulus convection on tropical climate system dynamics we refer to [25].

5 Discussion

Retaining the area fraction in the convective mass flux has been shown here to have far reaching implications for the boundary layer equilibrium state. In effect this corresponds to allowing for more

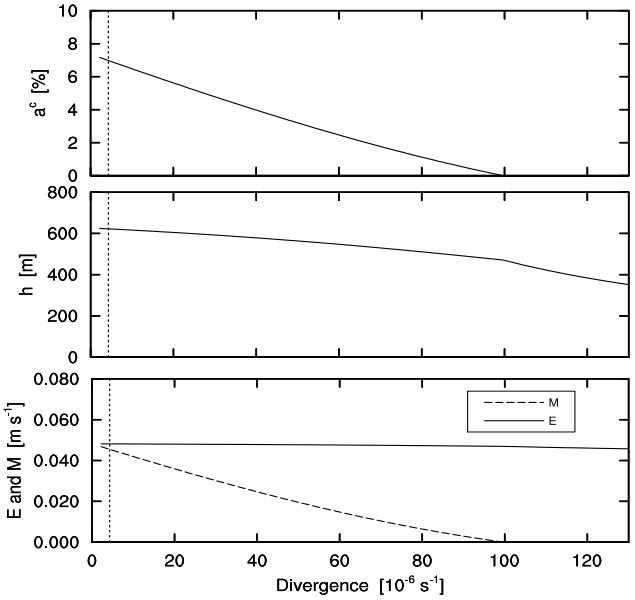

Fig. 10 Sensitivity test for the large-scale divergence D in the BOMEX case. a) Convective area fraction a^c, b) mixed layer top h, and c) entrainment E and mass flux M. The value of D in the standard BOMEX case is indicated by the dotted line.

degrees of freedom in the convective mass flux than is the case in many existing bulk closure techniques used in general circulation models and numerical weather prediction models [23]. Representing more degrees of freedom in the mass flux can be achieved by using a varying area fraction in a single bulk scheme, as is done in this model, or by employing an ensemble of updrafts.

The equilibrium solution features a smooth gradual increase of convective area fraction and mass flux along the tradewind trajectory. This is accompanied by an increasing surface evaporation field. Accordingly, the model suggests an explanation for the onset of cumulus convection during the boundary layer transition process. This is illustrated by a sensitivity test for large scale divergence in the BOMEX case, see Fig. 10. While in reality several parameters vary along the trajectory, the onset of shallow convection still occurs when a single boundary condition changes, which is helpful to gain insight into this problem. For subsidence conditions sufficiently stronger than the standard BOMEX case, $w = -Dh$ is large enough even with smaller h to balance the mass budget (1) without surface driven thermals ever reaching saturation ($E = -w, M = 0$). In this case this happens when $D > 1\mathrm{e}^{-4}$ s^{-1}, see Fig. 10 a) and b). Further downstream along the Tradewind trajectory, subsidence gets weaker, and the mixed layer has to grow deeper to reach the balance $E = Dh$. This brings surface driven thermals closer to condensation at mixed layer top, due to the decreasing q_{sat} with height. At some point along the trajectory, condensation will finally happen and cumulus onset occurs, see Fig. 10 a). The change in growth rate of h after cumulus onset reflects the relatively strong sensitivity of cumulus mass flux for a^c and its strong impact in the mass budget. The relatively large change in M compared to the small change in E across the range from large a^c to zero a^c is shown in Fig. 10 c).

While this is the basic mechanism behind the smooth onset of shallow cumulus, its exact location is also affected by other parameters. First, changing tropospheric humidity q_t^+ along the Tradewind trajectory affects both $\left(q_t^+ - q_t^1\right)$ and E (through the buoyancy jump), which changes the top entrainment flux in the humidity budget (5). The mixed layer thus reaches different humidity, affecting the saturation deficit at h and with it a^c. The same is true for θ^+. This implies that to understand boundary layer cloud climatology the characteristics of the overlying free troposphere should be taken into account. Second, the cloud transfer coefficients C_q^c and C_θ^c affect the mass flux in a similar way. Third, in reality the surface boundary conditions change significantly along the Tradewind trajectory, affecting the surface fluxes. Fourth, the forcing tendencies of radiation and advection may vary too, affecting the mixed layer budgets. Finally, it is important to note that a^c is significantly affected by the changing humidity variance at h. Figure 7 shows that the variance increases along the trajectory,

which is mainly caused by the more intense surface driven thermals that overshoot at h. Through the normalized saturation deficit this affects the convective area fraction, see (12).

Retaining a flexible area fraction in the mass flux makes the model in some aspects analogous to those of [8] and [1] as shown earlier. However, a major difference and novelty is the closure of that area fraction using a statistical framework, in which the saturation deficit and turbulent humidity variance appear. Statistical closures have been inspired by LES [35,13]. The use of these closures in this equilibrium model setting to understand climatology illustrates the potential use of high-resolution numerical modelling in atmospheric boundary layer research. This also puts previous models in the context of new LES findings.

Stratocumulus physics, such as cloud top radiative cooling, are not included in this model. Also note that a transition layer jump needs to exist for this model to be applicable. Observations have revealed that the decoupling level that develops below stratocumulus in the transition process later becomes shallow cumulus cloud base [2]. Accordingly, to match this bulk model with stratocumulus models, it needs to be known if decoupling takes place. As surface driven convection plays an important role in establishing decoupling, and our model only takes surface driven convection into account, it is not obvious here what is cause and what is effect. More work needs to be done to fully understand these interactions. At least the increasing surface evaporation along the tradewind trajectory in this model is consistent with the stratocumulus model of [10].

For simplicity cloud layer transport has been linearized in this model, to isolate the dominant role of the bulk mixed layer budgets in the shallow cumulus capped boundary layer. As entrainment E depends on the buoyancy jump at h, the cloud transfer coefficients C_q^c and C_θ^c affect the final equilibrium state of the mass flux. This was confirmed by a sensitivity test (not shown). The logical next step is therefore to include a more sophisticated cloud transport scheme in the model, to make it more generally applicable.

The model equilibrium can be solved for as an implicit system of algebraic equations using standard iterative techniques. Skipping the storage terms in the prognostic equations (1), (5) and (6) gives a set of simultaneous equations. The solution of this system (not shown) corresponds exactly to the final equilibrium state that is reached in the time dependent model.

In bulk models the mass flux does not appear in the prognostic budget equations for humidity and temperature. However, in multi-layer discretized models, such as single column models used in numerical weather prediction and climate models, mixed layer height h can fall in between gridpoints. As the associated tendencies reflect the changing boundary layer height, the mass flux then appears in the $\{q_t, \theta_l\}$ budget equations. This does not change the nature of the feedback mechanisms as present in the current model. A boosted mass flux at cloud base would quickly decrease humidity in the layer, in effect lowering mixed layer height.

6 Conclusions

A simple bulk model is formulated for the shallow cumulus topped mixed layer. The essential novelty in the approach is that the convective area fraction is retained in the mass flux closure. This fraction now depends on the state of the system, being a function of humidity and variance at mixed layer top. This represents an extra degree of freedom in the convective mass flux, and introduces a strong negative feedback in the system of equations. We call this mechanism the mass flux - humidity feedback. It is shown here to help determine the character of the equilibrium such that mixed layer top is always maintained close to lifting condensation level. This condition was used as a constraint in previous equilibrium models [8,1].

The model reproduces the basic characteristics of the convective area fraction and mass flux, boundary layer structure, turbulent thermodynamic variances, and the surface latent and sensible heat fluxes, as observed in nature, LES and ERA40. The cloud state and the surface fluxes are difficult aspects of convective boundary layers to reproduce, and therefore are a good indicator of model performance. The stability of the equilibrium state is corroborated by the observed persistent presence of shallow cumulus in the Tradewind regions.

These results show that the climatology of shallow cumulus capped boundary layers in the Trades can be explained by the subcloud mixed layer budgets. Such tight coupling of moist convection to subcloud layer or surface layer properties has been used in other recent modelling efforts [6,12]. In

addition to bulk mixed layer properties, the characteristics of the transition layer at cumulus cloud base are taken into account through the local saturation deficit and turbulent variance that appear in the statistical closure for the convective area fraction. The bulk subcloud layer properties that determine the saturation characteristics of the transition layer, and thus the area fraction of shallow cumulus, act as a regulator or valve on the moist convective transport. This is due to the strong sensitivity of the mass flux to the cloud fraction, as illustrated by the perturbation analysis for the BOMEX case. The robustness of the system is quantified by the associated modest perturbation in mixed layer depth.

The simple formulation of the mass flux model makes it potentially useful for climate modelling purposes. The associated long integration times require simple but accurate parameterizations of subgrid processes. The interactive climate run of the QTCM model featuring this mass flux model shows that on climatological timescales the extra degree of freedom in the mass flux closure always acts to keep the boundary layer close to the natural equilibrium state. In climate predictions cloud representation remains one of the most significant sources of uncertainty, and accordingly the representativeness of the equilibrium state of cloudiness as implied by parameterizations should receive much attention. We hope that this model can provide some more insight in this problem.

Acknowledgements This research was supported in part by National Science Foundation grants DMS-0139666 and ATM-0082529. The members of the Focused Research Group on tropical atmospheric dynamics are thanked for numerous discussions that helped stimulate this research. We thank Joel R. Norris for providing the figure of the climatological frequency of occurrence of marine shallow cumulus.

References

1. Albrecht, B. A., A. K. Betts, W. H. Schubert and S. K. Cox, 1979: A model of the thermodynamic structure of the Trade-wind boundary layer. Part I: Theoretical formulation and sensitivity tests. *J. Atmos. Sci.*, **36**, 73-89.
2. Albrecht, B. A., C. S. Bretherton, D. Johnson, W. H. Schubert, and A. S, Frisch, 1995: The Atlantic Stratocumulus Transition Experiment - ASTEX. *Bull. Amer. Met. Soc.*, **76**, 889-904.
3. Anthes, R. A., and D. Keyser, 1979: Tests of a fine-mesh model over Europe and the United States. *Mon. Wea. Rev.*, **107**, 963-984.
4. Augstein, E., H. Riehl, F. Ostapoff and V. Wagner, 1973: Mass and energy transports in an undisturbed Atlantic trade-wind flow. *Mon. Wea. Rev.*, **101**, 101-111.
5. Augstein, E., H. Schmidt and V. Wagner, 1974: The vertical structure of the atmospheric planetary boundary layer in undisturbed Trade winds over the Atlantic Ocean. *Bound.-Layer Meteor.*, **6**, 129-150.
6. Berg, L. K., and R. B. Stull, 2004: Parameterization of joint frequency distributions of potential temperature and water vapor mixing ratio in the daytime convective boundary layer. *J. Atmos. Sci.*, **61**, 813-828.
7. Betts, A. K., 1973: Non-precipitating cumulus convection and its parameterization. *Quart. J. Roy. Met. Soc.*, **99**, 178-196.
8. Betts, A. K., 1976: Modeling subcloud layer structure and interaction with a shallow cumulus layer. *J. Atmos. Sci.*, **33**, 2363-2382.
9. Betts, A. K., and W. Ridgway, 1989: Climatic equilibrium of the atmospheric convective boundary layer over the tropical ocean. *J. Atmos. Sci.*, **46**, 2621-2641.
10. Bretherton, C. S., and M. C. Wyant, 1997: Moisture transport, lower-tropospheric stability, and decoupling of cloud-topped boundary layers. *J. Atmos. Sci.*, **54**, 148-167.
11. Brown, A. R., A. Chlond, C. Golaz, M. Khairoutdinov, D. C. Lewellen, A. P. Lock, M. K. MacVean, C-H. Moeng, R. A. J. Neggers, A. P. Siebesma and B. Stevens, 2002: Large-eddy simulation of the diurnal cycle of shallow cumulus convection over land. *Quart. J. Roy. Met. Soc.*, **128**, 1075-1094.
12. Cheinet, S., 2004: A multiple mass flux parameterization for the surface-generated convection.Part II: Cloudy cores. *J. Atmos. Sci.*, **61**, 1093-1113.
13. Cuijpers, H., and P. Bechtold, 1995: A simple parameterization of cloud water related variables for use in boundary layer models. *J. Atmos. Sci.*, **52**, 2486-2490.
14. Cuijpers, H., and P. G. Duynkerke, 1993: Large-eddy simulation of trade-wind cumulus clouds. *J. Atmos. Sci.*, **50**, 3894-3908.
15. Deardorff, J. W., 1970: Convective velocity and temperature scales for the unstable planetary boundary layer and for Rayleigh convection. *J. Atm. Sci.*, **27**, 1211-1212.
16. Garratt, J. R., 1977: Review of drag coefficients over oceans and continents. *Mon. Wea. Rev.*, **105**, 915-929.
17. Grant, A. L. M., and A. R. Brown, 1999: A similarity hypothesis for shallow-cumulus transports. *Quart. J. Roy. Met. Soc.*, **125**, 1913-1936.
18. Grant, A. L. M., 2001: Cloud-base fluxes in the cumulus-capped boundary layer. *Quart. J. Roy. Met. Soc.*, **127**, 407-422.
19. Holland, J. Z., and E. M. Rasmusson, 1973: Measurement of atmospheric mass, energy and momentum budgets over a 500-kilometer square of tropical ocean. *Mon. Wea. Rev.*, **101**, 44-55.

20. Lenderink, G., Siebesma, P., Cheinet, S., Irons, S., Jones, C. G., Marquet, P., Müller, F., Olmeda, D., Calvo, J., Sanchez, E. and Soares, P. M. M., 2004: The diurnal cycle of shallow cumulus clouds over land: A single column model intercomparison study. *Q. J. Roy. Met. Soc.*, **130**, 3339-3364.
21. Lilly, D. K., 1968: Models of cloud-topped mixed layers under a strong inversion. *Q. J. Roy. Met. Soc.*, **84**, 292-309.
22. Neelin, J. D., and N. Zeng, 2000: A quasi-equilibrium tropical circulation model — formulation. *J. Atmos. Sci.*, **57**, 1741-1766.
23. Neggers, R. A. J., A. P. Siebesma, G. Lenderink and A. A. M. Holtslag: An evaluation of mass flux closures for diurnal cycles of shallow cumulus. *Mon. Wea. Rev.*, **132**, 2525-2538.
24. Neggers, R. A. J., B. Stevens, and J. D. Neelin, 2005a: Variance scaling in shallow cumulus topped mixed layers. *To be submitted to Q. J. Roy. Met. Soc., August 2005.*
25. Neggers, R. A. J., J. D. Neelin, and B. Stevens, 2005b: Impact mechanisms of shallow cumulus convection on tropical climate dynamics. *To be submitted to the Journal of Climate, August 2005.*
26. Nicholls, S., and M. A. LeMone, 1980: The fair weather boundary layer in GATE: the relationship of subcloud fluxes and structure to the distribution and enhancement of cumulus clouds. *J. Atmos. Sci.*, **37**, 2051-2067.
27. Nitta, T. and S. Esbensen, 1974: Heat and moisture budget analyses using BOMEX data. *Mon. Wea. Rev.*, **102**, 17-28.
28. Norris, J. R., 1998: Low cloud type over the ocean from surface observations. Part II: Geographical and seasonal variations. *J. Clim.*, **11**, 383-403.
29. Ooyama, K., 1971: A theory on parameterization of cumulus convection. *J. Meteor. Soc. Japan*, **49**, 744-756.
30. Riehl, H., C. Yeh, J. S. Malkus, and N. E. LaSeur, 1951: The northeast trade of the Pacific Ocean. *Quart. J. Roy. Meteor. Soc.*, **77**, 598-626.
31. Schubert, W. H., 1976: Experiments with Lilly's cloud-topped mixed layer model. *J. Atm. Sci.*, **33**, 436-446.
32. Siebesma, A. P., C. S. Bretherton, A. Brown, A. Chlond, J. Cuxart, P. G. Duynkerke, H. Jiang, M. Khairoutdinov, D. Lewellen, C.-H. Moeng, E. Sanchez, B. Stevens, and D. E. Stevens, 2003: A large eddy simulation intercomparison study of shallow cumulus convection. *J. Atmos.Sci.*, **60**, 1201-1219.
33. Siebesma, A. P., C. Jakob, G. Lenderink, R. A. J. Neggers, J. Teixeira, E. Van Meijgaard, J. Calvo, A. Chlond, H. Grenier, C. Jones, M. Koehler, H. Kitagawa, P.Marquet, A. P. Lock, F. Muller, D. Olmeda and C. Severijns, 2004: Cloud representation in general-circulation models over the northern Pacific Ocean: A EUROCS intercomparison study. *Q. J. R. Meteorol. Soc.*, **130**, 1-23.
34. Siebesma, A. P., and Cuijpers, 1995: Evaluation of parametric assumptions for shallow cumulus convection. *J. Atmos. Sci.*, **52**, 650-666.
35. Sommeria, G., and J. W. Deardorff, 1977: Subgrid-scale condensation in models of non-precipitating clouds. *J. Atmos. Sci.*, **34**, 344-355.
36. Stevens, B., A. S. Ackerman, B. A. Albrecht, A. R. Brown, A. Chlond, J. Cuxart, P. G. Duynkerke, D. C. Lewellen, M. K. MacVean, R. A. J. Neggers, E. Sanchez, A. P. Siebsema, D. E. Stevens, 2001: Simulations of Trade-wind cumuli under a strong inversion. *J. Atmos. Sci.*, **58**, 1870-1891.
37. Stevens, B., 2005: Boundary layer concepts for simplified models of tropical dynamics. *Theoret. Comput. Fluid Dynamics*, Submitted.
38. Stull, R. B., 1988: *An introduction to boundary layer meteorology*, Kluwer Academic Publishers, The Netherlands. 670pp.
39. Yanai, M., S. Esbensen and J. H. Cho, 1973: Determination of bulk properties of tropical cloud clusters from large-scale heat and moisture budgets. *J. Atmos. Sci.*, **30**, 611-627.
40. Yin, B., and B. A. Albrecht, 2000: Spatial variability of atmospheric boundary layer structure over the eastern equatorial Pacific. *J. Clim.*, **13**, 1574-1592.